Supporting Information

Lack et al. 10.1073/pnas.1206575109

SI Text

Measurement Methods. The photo-acoustic response to absorption at all wavelengths is calibrated using CRDS as an absolute measure of ozone absorption (O_3 generated using ultra-zero air through an O_3 generator) (1).

The SP2 was calibrated over a BC mass range of 1–15 fg, (approximately 100–250 nm volume-equivalent diameter) with fullerene soot (Alfa Aesar, Inc.). Over the size range of most of the BC in the accumulation mode, the calibration is very close to purely linear. Fullerene soot is being accepted as the standard material for absolute and relative calibration of SP2s (2) and has shown to be an excellent reference material for ambient BC (3, 4).

Primary Data. Fig. S1 shows a time series of measured extinction (660, 532, 405 nm), absorption (658, 532, 404 nm), POM mass, nonrefractory particle mass (NR-PM), which includes POM and ammonium nitrate, and BC mass.

Definition of Time Periods. See Table S2.

Chemical Signature of Biomass Burning Particles. See Fig. S2.

Optical Properties: Absorption Angstrom Exponent and Single Scattering Albedo. The absorption angstrom exponent (AAE), fit to non-denuded 404, 532, and 658 nm PAS data, shows average values ranging from 1.25 to 2.5 (Fig. S3 *A* and *B*). These values are similar to the AAEs presented for biomass combustion particles of Gyawali et al. (5) and Lewis et al. (6) and indicate substantial additional absorption at 404 nm.

During the *BB1* period, the SSA_{532} and SSA_{658} are stable at approximately 0.90 while the SSA_{404} is stable at a lower value, approximately 0.85. That SSA_{532} and SSA_{658} are so similar provides evidence that there is minimal POM absorption at 532 nm. Although the data presented in the main manuscript suggests that there is significant contribution to absorption by BrC and lensing, the SSA of the particles actually increased as the m_{POM} increased, an indication that the scattering efficiency of the BrC is larger than the absorption efficiency. Interestingly, the SSA was relatively stable during the period (*BB1*) and decreased and became highly variable during period (*BB2*). Lewis et al. (6) measured the SSA of many different biomass fuel types and found large differences amongst fuels. Their SSA_{404} for Ponderosa Pine combustion particles of approximately 0.87 compares to the average SSA_{404} of 0.85 during the *BB* period of this fire. Our SSA data is also consistent with the emissions from smoldering boreal forest fires reported in a range of other studies (7, 8) (Fig. S3).

AMS Mass Balance. The nonrefractory PM emitted during the fire (measured by the AMS) was consistently comprised of 90% POM and 10% ammonium nitrate (Fig. S8). A very good closure between the calculated ammonium (ammonium required to balance out the measured nitrate) and the measured ammonium indicates that the reported nitrate is predominantly ammonium nitrate. The excess signal at m/z 30 was a small fraction (<3%) of the reported organic mass. Based on previous ambient measurements, observing high ammonium nitrate concentrations in biomass burning plumes is not surprising (9) because NH_3 and NO_X emissions from fires can be high (10). Losses of ammonium nitrate mass in the PAS and CRD instruments due to drying of the aerosol (i.e., ammonium nitrate gas/particle equilibrium) will be minimal. The sample flow in the PAS and CRD systems was dried to &*lt*;= 25% RH prior to measurement while the average and maximum ambient RHs were 28% and 46%, respectively (11) (Fig. S8).

Calculation of Count Median Diameters from AMS. Vacuum aerodynamic diameters of the AMS mass size distribution (d_{MVA}) were converted to a volume equivalent diameter (d_{VVA}) by dividing d_{MVA} by an assumed POM/ammonium nitrate density. The volume per particle size bin was calculated from d_{VVA}. The mass concentration ($\mu g\,m^{-3}$) in each size bin was converted to volume concentration ($m^3\,m^{-3}$) by applying the assumed density. The volume concentration divided by volume per particle produces the count equivalent size distribution, to which a log-normal function is fit. The assumed density of NR-PM was $1.4(\pm 0.1)\,g\,cm^{-3}$ (12).

Internal vs external mixing. Graphical representation of the calculation procedure for coating growth factor (CF) and mass fraction of externally mixed PM ($f_{POM\text{-}Ext}$) and POM ($f_{POM\text{-}Ext}$):

Fig. S4 shows a schematic of the assumptions made within the modeling process to determine optimal CF and $f_{POM\text{-}Ext}$. Fig. S5 illustrates the CF optimization and $f_{POM\text{-}Ext}$ calculation procedure.

SP2 estimate of internal vs. external mixing. The specific instrumental setup of the SP2 in conjunction with the size range of the aerosols under study determine the ability of the SP2 to provide meaningful information about the mixing state of total aerosol vis-a-vis BC. Here, the SP2 was not optimized to provide either a best estimate of the number concentration of BC-containing particles or to determine total particle concentration. The SP2 is able to provide measures of both the number concentration of BC cores above a given diameter (here approximately 100 nm volume equivalent, VED), and the number concentration of particles without detectable BC (i.e., <100 nm BC VED) that are larger than a given optical size (here 200 nm). As a large fraction of the total number of all aerosol (those with and without BC content) is contained in sizes below the SP2 optical size limit, and potentially a large fraction of the total number of all BC cores, these values are semi-quantitative and should be used with caution.

Calculation of BrC imaginary RI. Graphical representation of the calculation procedure for the imaginary refractive index of brown carbon. See Fig. S6.

Attribution of absorption / mass absorption efficiency. Graphical representation of the calculation procedure for mass absorption efficiency. See Fig. S7.

1. Lack D, et al. (2012) Aircraft instrumentation for comprehensive characterization of aerosol optical properties, Part 2: Black and brown carbon absorption and absorption enhancement measured with photo acoustic spectroscopy. *Aerosol Sci Technol* 46:555–568.
2. Laborde M, et al. (2012) Single particle soot photometer intercomparison at the AIDA chamber. *Atmos Meas Tech Discuss* 5:3519–3573.
3. Laborde M, et al. (2012) Sensitivity of the single particle soot photometer to different black carbon types. *Atmos Meas Tech* 5:1031–1043.
4. Moteki N, Kondo Y (2010) Dependence of laser-induced incandescence on physical properties of black carbon aerosols: Measurements and theoretical interpretation. *Aerosol Sci Technol* 44:663–675.
5. Gyawali M, Arnott WP, Lewis K, Moosmuller H (2009) In situ aerosol optics in Reno, NV, USA during and after the summer 2008 California wildfires and the influence of absorbing and non-absorbing organic coatings on spectral light absorption. *Atmos Chem Phys* 9:8007–8017.

6. Lewis K, Arnott WP, Moosmuller H, Wold CE (2008) Strong spectral variation of biomass smoke light absorption and single scattering albedo observed with a novel dual-wavelength photoacoustic instrument. *J Geophys Res* 113:D16203.
7. Abel SJ, Haywood JM, Highwood EJ, Li J, Buseck PR (2003) Evolution of biomass burning aerosol properties from an agricultural fire in southern Africa. *Geophys Res Lett* 30:1783–1786.
8. Reid JS, et al. (2005) A review of biomass burning emissions part III: Intensive optical properties of biomass burning particles. *Atmos Chem Phys* 5:827–849.
9. Brock CA, et al. (2011) Characteristics, sources, and transport of aerosols measured in spring 2008 during the aerosol, radiation, and cloud processes affecting Arctic Climate (ARCPAC) Project. *Atmos Chem Phys* 11:2423–2453.
10. Andreae MO, Merlet P (2001) Emission of trace gases and aerosols from biomass burning. *Global Biogeochem Cycles* 15:955–966.
11. NOAA (2010) Historical Meterological Data for Boulder, CO. (NOAA National Climatic Data Center). Available at www.ncdc.noaa.gov.
12. Alfarra MR, et al. (2006) A mass spectrometric study of secondary organic aerosols formed from the photo- oxidation of anthropogenic and biogenic precursors in a reaction chamber. *Atmos Chem Phys* 6:5279–5293.
13. Cubison MJ, et al. (2011) Effects of aging on organic aerosol from open biomass burning smoke in aircraft and lab studies. *Atmos Chem Phys* 11:1680–7324.

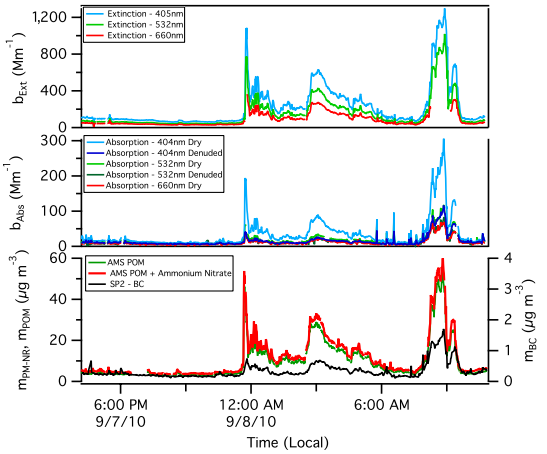

Fig. S1. Time series of extinction, absorption, AMS-measured mass (PM-NR and POM) and SP2-measured BC.

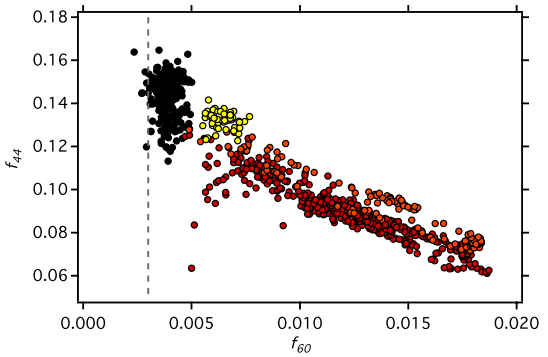

Fig. S2. AMS fraction of m_{POM} as m/z 44 vs m/z 60 colored by the periods identified in Table 1 and Fig. 1*A* in the main manuscript. Urban background f60 from Cubison et al. (13) shown as vertical dashed line.

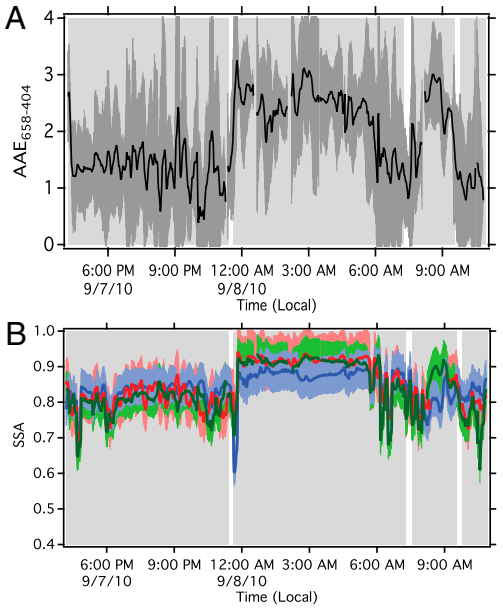

Fig. S3. (*A*) $AAE_{404–658}$ time series and (*B*) particle single scatter albedo vs. time. 658 nm, red; 532 nm, green; 404 nm, blue. Shaded regions surrounding main data indicate 1 Hz data.

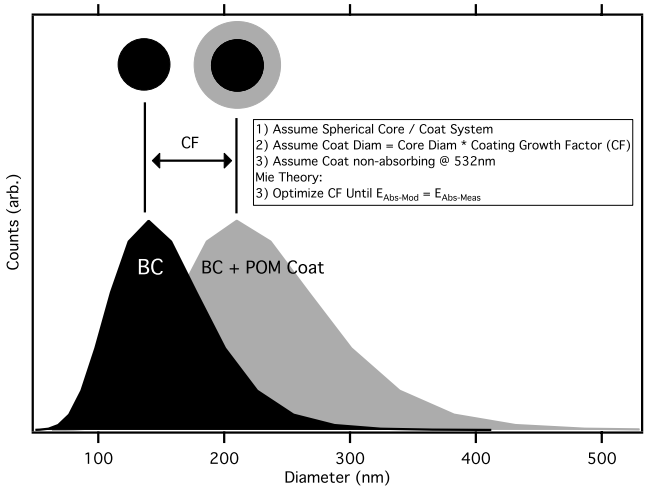

Fig. S4. Schematic of assumptions made to determine of external mixing of POM.

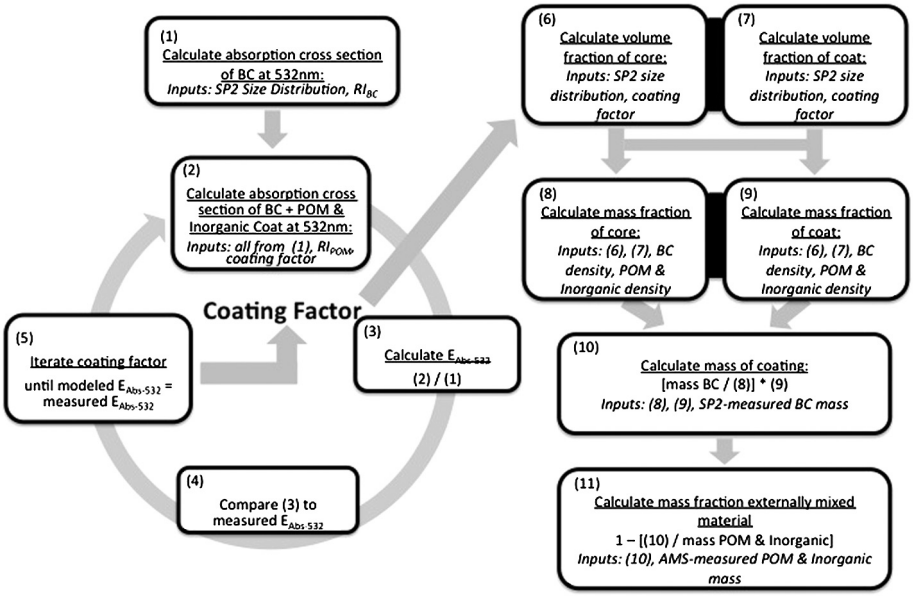

Fig. S5. Optimization process for coating growth factor (CF) determination and the calculation process for $f_{PM-NR-Ext}$ and $f_{POM-Ext}$.

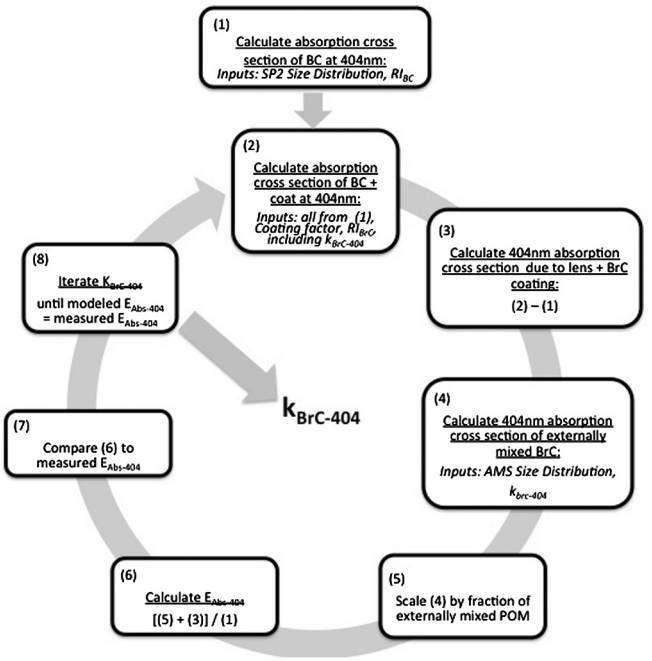

Fig. S6. Optimization process for the calculation of BrC imaginary refractive index ($k_{BrC-404}$).

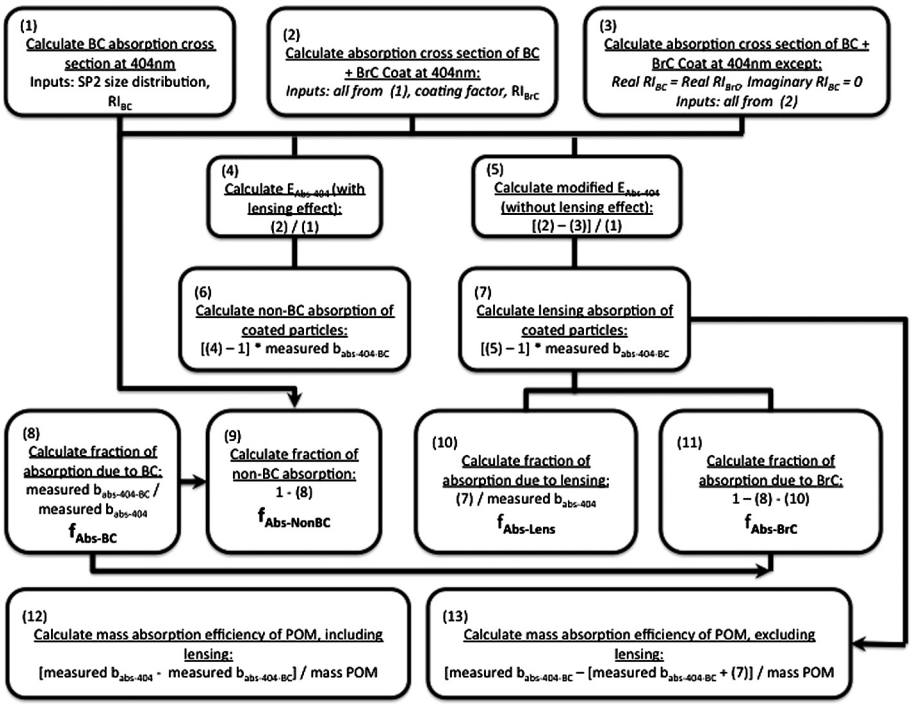

Fig. S7. Calculation procedure for the partitioning of absorption between BC, BC-lensing and BrC, in addition to the calculation of the mass absorption efficiency.

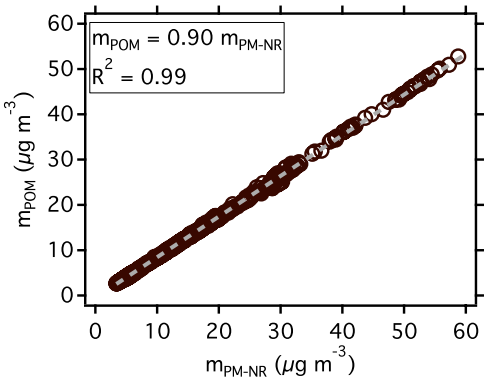

Fig. S8. AMS-measured total mass ($m_{\text{PM-NR}} = m_{\text{POM}} + m_{\text{ammonium nitrate}}$) vs. m_{POM}.

Table S1. Abbreviations and definitions used in this study

Parameter / Abbreviation	Definition
$b_{\text{Abs-658}}$, $b_{\text{Abs-532}}$, $b_{\text{Abs-404}}$	Photo-acoustic measured absorption at 658, 532, 404 nm
$b_{\text{Abs-532-BC}}$, $b_{\text{Abs-404-BC}}$	Photo-acoustic measured absorption of thermal-denuded sample at 532, 404 nm
$b_{\text{Abs-532-Lens}}$, $b_{\text{Abs-404-Lens}}$	Absorption due to internal mixing of BC and NR-PM at 532, 404 nm
$b_{\text{Abs-404-BrC}}$	Absorption due to intrinsic absorption of POM at 404 nm
$b_{\text{Ext-660}}$, $b_{\text{Ext-532}}$ $b_{\text{Ext-405}}$	Cavity ring down measured absorption at 660, 532, 405 nm
BB	Biomass burning
BB1, BB2	Biomass burning influenced sampling periods 1 and 2
BC	Black carbon
BG1, BG2	Atmospheric background periods 1 and 2
BrC	Brown carbon
CF	Coating growth factor
d_{Core}	Diameter of BC core used in Mie modeling
d_{Total}	Diameter of BC core and coating used in Mie modeling
$E_{\text{Abs-532}}$, $E_{\text{Abs-404}}$	Absorption enhancement at 532 nm/404 nm
$E_{\text{Abs-404-All-Mod}}$	Modeled absorption enhancement at 404 nm
$E_{\text{Abs-404-NoBrC-Mod}}$	Modeled absorption enhancement at 404 nm with intrinsic absorption of POM removed

Parameter / Abbreviation	Definition
f_{44}, f_{60}	Fraction of POM that is comprised of AMS mass to charge fragment 44/60
$f_{Abs\text{-}BC}$	Fraction of absorption sourced from BC
$f_{Abs\text{-}BrC}$	Fraction of absorption sourced from BrC
$f_{Abs\text{-}Lens}$	Fraction of absorption sourced from internal mixing
$f_{Abs\text{-}NonBC}$	Fraction of absorption sourced from internal mixing and BrC
f_{BC}	Fraction of modeled internally mixed particle mass that is BC
FF	Fossil fuel
$f_{PM\text{-}NR}$	Fraction of modeled internally mixed particle mass that is NR-PM
$f_{PM\text{-}NR\text{-}Ext}$	Fraction of mass of NR-PM externally mixed (not associated with a BC core)
$f_{POM\text{-}Ext}$	Fraction of mass of POM externally mixed (not associated with a BC core)
$k_{BrC\text{-}404}$	Imaginary RI of POM (brown carbon) at 404 nm
MAE_{BrC}	Mass absorption efficiency (also called mass absorption coefficient) of BrC at 404 nm
$MAE_{BrC\text{-}Lens}$	Mass absorption efficiency of BrC at 404 nm including effect of internal mixing
M_{BC}	SP2-measured mass of BC
m_{POM}	AMS-measured mass of POM
$m_{PM\text{-}NR}$	AMS-measured mass of NR-PM
$m_{PM\text{-}NR\text{-}Int}$	Mass of NR-PM internally mixed with BC
NR-PM	Non-refractory particulate mass. POM + ammonium nitrate
POM	AMS measured particulate organic matter
RI	Complex refractive index
$\sigma_{Abs\text{-}404\text{-}BC\text{-}Lens\text{-}BrC}$	Modeled absorption cross-section of BC coated in POM at 404 nm. Includes absorption from BC, internal mixing (lens) and intrinsic POM absorption.
$\sigma_{Abs\text{-}404\text{-}BrC\text{-}Ext}$	Modeled absorption cross-section of externally mixed POM at 404 nm.
$\sigma_{Abs\text{-}404\text{-}BrC\text{-}Int}$	Modeled absorption cross-section of internally mixed POM at 404 nm. No effect of internal mixing
$\sigma_{Abs\text{-}404\text{-}BrC\text{-}Ext\text{-}Scaled}$	Modeled absorption cross-section of externally mixed POM at 404 nm scaled by the volume ratio of externally mixed to internally mixed POM
$\sigma_{Abs\text{-}404\text{-}BC}$	Modeled absorption cross-section of BC at 404 nm

Table S2. Definition and description of sampling periods within this study

Period	$E_{Abs\text{-}532}$	$E_{Abs\text{-}404}$	POM Mass ($\mu g\ m^{-3}$)
BG1 **Background/Low Signal** Daytime/Nighttime (black data, Fig. 1 *B* and *C*)	1.0–1.5 Consistent with BC coated in nonabsorbing POM (1)	1.3–1.7	0.0–5.0
BB1 **Biomass Burning Dominated** Nighttime (brown data, Fig. 1 *B* and *C*)	1.4 ± 0.1 Consistent with POM coated BC with enhanced absorption by lensing	Ranging up to 3.5 Consistent with intrinsic POM absorption at 404 nm	>5.0
BB2 **Biomass Burning-Anthropogenic** Sunrise/Morning traffic emissions (orange data, Fig. 1 *B* and *C*)	1.4 ± 0.1 Consistent with POM coated BC with enhanced absorption by lensing	1.5–2.5 Indicates an increase in BC concentrations and /or an increase in POM coatings that do not absorb (at 404 nm) as much as period 2.	>5.0
BG2 **Background/Low Signal** Daytime (yellow data, Fig. 1 *B* and *C*)	1.0–1.5 Consistent with BC coated in nonabsorbing POM (1)	1.3–1.7	0.0–5.0